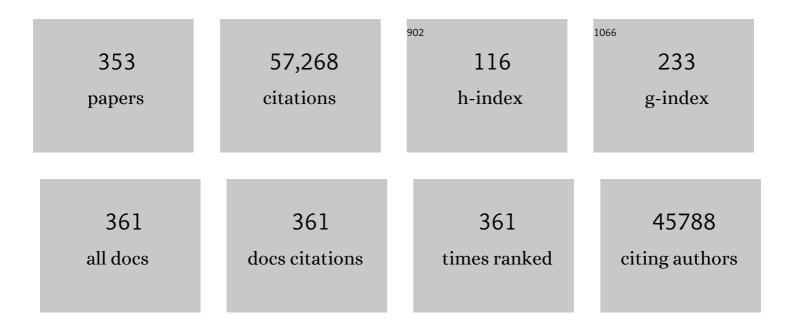
## List of Publications by Year in descending order

Source: https://exaly.com/author-pdf/1060048/publications.pdf Version: 2024-02-01



ALLIANEY

#	Article	lF	CITATIONS
1	Engineering Exciton Recombination Pathways in Bilayer WSe <sub>2</sub> for Bright Luminescence. ACS Nano, 2022, 16, 1339-1345.	7.3	18
2	Orientated Growth of Ultrathin Tellurium by van der Waals Epitaxy. Advanced Materials Interfaces, 2022, 9, .	1.9	7
3	Bright Mid-Wave Infrared Resonant-Cavity Light-Emitting Diodes Based on Black Phosphorus. Nano Letters, 2022, 22, 1294-1301.	4.5	19
4	Tanks and Truth. ACS Nano, 2022, 16, 4975-4976.	7.3	0
5	Resettable Microfluidics for Broad-Range and Prolonged Sweat Rate Sensing. ACS Sensors, 2022, 7, 1156-1164.	4.0	23
6	Enhanced Neutral Exciton Diffusion in Monolayer WS <sub>2</sub> by Exciton–Exciton Annihilation. ACS Nano, 2022, 16, 8005-8011.	7.3	11
7	Theory of liquid-mediated strain release in two-dimensional materials. Physical Review Materials, 2022, 6, .	0.9	1
8	Efficiency Roll-Off Free Electroluminescence from Monolayer WSe <sub>2</sub> . Nano Letters, 2022, 22, 5316-5321.	4.5	11
9	Structural heterogeneity in non-crystalline Te <sub><i>x</i></sub> Se1â^²x thin films. Applied Physics Letters, 2022, 121, 012101.	1.5	1
10	Laserâ€Assisted Thermomechanical Thinning of MoTe <sub>2</sub> in Nanoscale Lateral Resolution. Advanced Materials Interfaces, 2022, 9, .	1.9	2
11	Wearable Biosensors for Body Computing. Advanced Functional Materials, 2021, 31, 2008087.	7.8	56
12	Performance Limits of an Alternating Current Electroluminescent Device. Advanced Materials, 2021, 33, e2005635.	11.1	11
13	A Wearable Nutrition Tracker. Advanced Materials, 2021, 33, e2006444.	11.1	70
14	Universal Inverse Scaling of Exciton–Exciton Annihilation Coefficient with Exciton Lifetime. Nano Letters, 2021, 21, 424-429.	4.5	20
15	Polarization-Converting Plasmonic Nanoantennas for Light Absorption Enhancement in Anisotropic 2D Black Phosphorus. , 2021, , .		0
16	Long-Wave Infrared Photodetectors Based on 2D Platinum Diselenide atop Optical Cavity Substrates. ACS Nano, 2021, 15, 6573-6581.	7.3	29
17	Light–Matter Interaction Enhancement in Anisotropic 2D Black Phosphorus via Polarization-Tailoring Nano-Optics. ACS Photonics, 2021, 8, 1120-1128.	3.2	20
18	A wearable patch for continuous analysis of thermoregulatory sweat at rest. Nature Communications, 2021, 12, 1823.	5.8	181

#	Article	IF	CITATIONS
19	Longwave Infrared Photoresponse in Copper 7,7,8,8-tetracyano-2,3,5,6-tetraflouroquinodimethane (CuTCNQF4). , 2021, , .		0
20	Inhibited nonradiative decay at all exciton densities in monolayer semiconductors. Science, 2021, 373, 448-452.	6.0	52
21	Tellurium Singleâ€Crystal Arrays by Lowâ€Temperature Evaporation and Crystallization. Advanced Materials, 2021, 33, e2100860.	11.1	32
22	Actively variable-spectrum optoelectronics with black phosphorus. Nature, 2021, 596, 232-237.	13.7	132
23	Copper Tetracyanoquinodimethane (CuTCNQ): A Metal–Organic Semiconductor for Room-Temperature Visible to Long-Wave Infrared Photodetection. ACS Applied Materials & Interfaces, 2021, 13, 38544-38552.	4.0	10
24	A Resonantly Driven, Electroluminescent Metal Oxide Semiconductor Capacitor with High Power Efficiency. ACS Nano, 2021, 15, 15210-15217.	7.3	10
25	Wearable Biosensors for Body Computing (Adv. Funct. Mater. 39/2021). Advanced Functional Materials, 2021, 31, 2170290.	7.8	8
26	Temperature-adaptive radiative coating for all-season household thermal regulation. Science, 2021, 374, 1504-1509.	6.0	251
27	Flexible Electrochemical Bioelectronics: The Rise of In Situ Bioanalysis. Advanced Materials, 2020, 32, e1902083.	11.1	200
28	Shape-controlled single-crystal growth of InP at low temperatures down to 220 °C. Proceedings of the United States of America, 2020, 117, 902-906.	3.3	8
29	Evaporated tellurium thin films for p-type field-effect transistors and circuits. Nature Nanotechnology, 2020, 15, 53-58.	15.6	153
30	Centimeterâ€Scale and Visible Wavelength Monolayer Lightâ€Emitting Devices. Advanced Functional Materials, 2020, 30, 1907941.	7.8	20
31	Molecular Materials with Short Radiative Lifetime for High-Speed Light-Emitting Devices. Matter, 2020, 3, 1832-1844.	5.0	10
32	Evaporated Se <i><sub>x</sub></i> Te <sub>1â€</sub> <i><sub>x</sub></i> Thin Films with Tunable Bandgaps for Shortâ€Wave Infrared Photodetectors. Advanced Materials, 2020, 32, e2001329.	11.1	49
33	A generic electroluminescent device for emission from infrared to ultraviolet wavelengths. Nature Electronics, 2020, 3, 612-621.	13.1	23
34	Glove-based sensors for multimodal monitoring of natural sweat. Science Advances, 2020, 6, eabb8308.	4.7	86
35	Neutral Exciton Diffusion in Monolayer MoS <sub>2</sub> . ACS Nano, 2020, 14, 13433-13440.	7.3	62
36	Thermal stability for Te-based devices. Applied Physics Letters, 2020, 117, .	1.5	12

#	Article	IF	CITATIONS
37	Nicotine Monitoring with a Wearable Sweat Band. ACS Sensors, 2020, 5, 1831-1837.	4.0	48
38	A biomimetic eye with a hemispherical perovskite nanowire array retina. Nature, 2020, 581, 278-282.	13.7	392
39	Extreme In-Plane Thermal Conductivity Anisotropy in Titanium Trisulfide Caused by Heat-Carrying Optical Phonons. Nano Letters, 2020, 20, 5221-5227.	4.5	21
40	Fully R2Râ€Printed Carbonâ€Nanotubeâ€Based Limitless Length of Flexible Activeâ€Matrix for Electrophoretic Display Application. Advanced Electronic Materials, 2020, 6, 1901431.	2.6	49
41	Integration of amorphous ferromagnetic oxides with multiferroic materials for room temperature magnetoelectric spintronics. Scientific Reports, 2020, 10, 3583.	1.6	16
42	Mid- to long-wave infrared computational spectroscopy with a graphene metasurface modulator. Scientific Reports, 2020, 10, 5377.	1.6	23
43	Polymeric Electron-Selective Contact for Crystalline Silicon Solar Cells with an Efficiency Exceeding 19%. ACS Energy Letters, 2020, 5, 897-902.	8.8	35
44	Anomalously Suppressed Thermal Conduction by Electronâ€Phonon Coupling in Chargeâ€Đensityâ€Wave Tantalum Disulfide. Advanced Science, 2020, 7, 1902071.	5.6	22
45	Flexible Electronics: Flexible Electrochemical Bioelectronics: The Rise of In Situ Bioanalysis (Adv.) Tj ETQq1 1 0.78	4314.rgB <sup>-</sup> 11.1	[ /Qverlock ]
46	Traceâ€Level, Multiâ€Gas Detection for Food Quality Assessment Based on Decorated Silicon Transistor Arrays. Advanced Materials, 2020, 32, e1908385.	11.1	77
47	Substrate-Dependent Exciton Diffusion and Annihilation in Chemically Treated MoS <sub>2</sub> and WS <sub>2</sub> . Journal of Physical Chemistry C, 2020, 124, 12175-12184.	1.5	51
48	Growing Contributions of Nano in 2020. ACS Nano, 2020, 14, 16163-16164.	7.3	1
49	Improved Hydrogen Sensitivity and Selectivity in PdO with Metal-Organic Framework Membrane. Journal of the Electrochemical Society, 2020, 167, 147503.	1.3	5
50	Long-Wave Infrared Photodetectors Based on Platinum Diselenide. , 2020, , .		0
51	Visible to Long-Wave Infrared Photodetectors based on Copper Tetracyanoquinodimethane (CuTCNQ) Crystals. , 2020, , .		0
52	Wearable Sweat Band for Noninvasive Levodopa Monitoring. Nano Letters, 2019, 19, 6346-6351.	4.5	121
53	A multi-modal sweat sensing patch for cross-verification of sweat rate, total ionic charge, and Na <sup>+</sup> concentration. Lab on A Chip, 2019, 19, 3179-3189.	3.1	56
54	Regional and correlative sweat analysis using high-throughput microfluidic sensing patches toward decoding sweat. Science Advances, 2019, 5, eaaw9906.	4.7	234

#	Article	IF	CITATIONS
55	Transistorâ€Based Workâ€Function Measurement of Metal–Organic Frameworks for Ultra‣owâ€Power, Rationally Designed Chemical Sensors. Chemistry - A European Journal, 2019, 25, 13176-13183.	1.7	18
56	Intrinsic Optoelectronic Characteristics of MoS <sub>2</sub> Phototransistors <i>via</i> a Fully Transparent van der Waals Heterostructure. ACS Nano, 2019, 13, 9638-9646.	7.3	43
57	Bright electroluminescence in ambient conditions from WSe2 p-n diodes using pulsed injection. Applied Physics Letters, 2019, 115, 011103.	1.5	13
58	A Fully Integrated and Self-Powered Smartwatch for Continuous Sweat Glucose Monitoring. ACS Sensors, 2019, 4, 1925-1933.	4.0	184
59	Scanning Probe Lithography Patterning of Monolayer Semiconductors and Application in Quantifying Edge Recombination. Advanced Materials, 2019, 31, e1900136.	11.1	27
60	Scalable Ultra Low-Power Chemical Sensing with Metal-Organic Frameworks. , 2019, , .		0
61	Two-Chip Wireless H2S Gas Sensor System Requiring Zero Additional Electronic Components. , 2019, , .		2
62	Gate Quantum Capacitance Effects in Nanoscale Transistors. Nano Letters, 2019, 19, 7130-7137.	4.5	6
63	Porous Enzymatic Membrane for Nanotextured Glucose Sweat Sensors with High Stability toward Reliable Noninvasive Health Monitoring. Advanced Functional Materials, 2019, 29, 1902521.	7.8	120
64	Optical and electrical properties of two-dimensional palladium diselenide. Applied Physics Letters, 2019, 114, .	1.5	74
65	Elimination of Response to Relative Humidity Changes in Chemical-Sensitive Field-Effect Transistors. ACS Sensors, 2019, 4, 1857-1863.	4.0	24
66	Electrical suppression of all nonradiative recombination pathways in monolayer semiconductors. Science, 2019, 364, 468-471.	6.0	243
67	Physical and Chemical Sensing With Electronic Skin. Proceedings of the IEEE, 2019, 107, 2155-2167.	16.4	56
68	In Situ Transmission Electron Microscopy Study of Molybdenum Oxide Contacts for Silicon Solar Cells. Physica Status Solidi (A) Applications and Materials Science, 2019, 216, 1800998.	0.8	6
69	Dip Coating Passivation of Crystalline Silicon by Lewis Acids. ACS Nano, 2019, 13, 3723-3729.	7.3	28
70	InAs FinFETs Performance Enhancement by Superacid Surface Treatment. IEEE Transactions on Electron Devices, 2019, 66, 1856-1861.	1.6	10
71	Increasing Photoluminescence Quantum Yield by Nanophotonic Design of Quantum-Confined Halide Perovskite Nanowire Arrays. Nano Letters, 2019, 19, 2850-2857.	4.5	67
72	Si photocathode with Ag-supported dendritic Cu catalyst for CO <sub>2</sub> reduction. Energy and Environmental Science, 2019, 12, 1068-1077.	15.6	93

#	Article	IF	CITATIONS
73	Spatially Precise Transfer of Patterned Monolayer WS <sub>2</sub> and MoS <sub>2</sub> with Features Larger than 10 <sup>4</sup> μm <sup>2</sup> Directly from Multilayer Sources. ACS Applied Electronic Materials, 2019, 1, 407-416.	2.0	23
74	Flexible Electronics toward Wearable Sensing. Accounts of Chemical Research, 2019, 52, 523-533.	7.6	713
75	In Situ Transmission Electron Microscopy: A Powerful Tool for the Characterization of Carrier-Selective Contacts. , 2019, , .		0
76	Monolayer Semiconductors: Scanning Probe Lithography Patterning of Monolayer Semiconductors and Application in Quantifying Edge Recombination (Adv. Mater. 48/2019). Advanced Materials, 2019, 31, 1970340.	11.1	0
77	Strong optical response and light emission from a monolayer molecular crystal. Nature Communications, 2019, 10, 5589.	5.8	59
78	Passivating contacts for crystalline silicon solar cells. Nature Energy, 2019, 4, 914-928.	19.8	374
79	Synthetic WSe <sub>2</sub> monolayers with high photoluminescence quantum yield. Science Advances, 2019, 5, eaau4728.	4.7	78
80	Dopantâ€Free Partial Rear Contacts Enabling 23% Silicon Solar Cells. Advanced Energy Materials, 2019, 9, 1803367.	10.2	77
81	Deterministic Assembly of Arrays of Lithographically Defined WS2 and MoS2 Monolayer Features Directly From Multilayer Sources Into Van Der Waals Heterostructures. Journal of Micro and Nano-Manufacturing, 2019, 7, .	0.8	12
82	Mid-Infrared Computational Spectroscopy with an Electrically-Tunable Graphene Metasurface. , 2019, , .		0
83	Ordered polymer-based spin-on dopants. , 2019, , .		1
84	Wearable sweat sensors. Nature Electronics, 2018, 1, 160-171.	13.1	947
85	Helmuth Möhwald (1946–2018). ACS Nano, 2018, 12, 3053-3055.	7.3	0
86	Methylxanthine Drug Monitoring with Wearable Sweat Sensors. Advanced Materials, 2018, 30, e1707442.	11.1	226
87	Highly Sensitive Bulk Silicon Chemical Sensors with Sub-5 nm Thin Charge Inversion Layers. ACS Nano, 2018, 12, 2948-2954.	7.3	41
88	Stable Dopant-Free Asymmetric Heterocontact Silicon Solar Cells with Efficiencies above 20%. ACS Energy Letters, 2018, 3, 508-513.	8.8	164
89	Cation-Dependent Light-Induced Halide Demixing in Hybrid Organic–Inorganic Perovskites. Nano Letters, 2018, 18, 3473-3480.	4.5	65
90	Large-area and bright pulsed electroluminescence in monolayer semiconductors. Nature Communications, 2018, 9, 1229.	5.8	146

#	Article	IF	CITATIONS
91	Tantalum Oxide Electron-Selective Heterocontacts for Silicon Photovoltaics and Photoelectrochemical Water Reduction. ACS Energy Letters, 2018, 3, 125-131.	8.8	127
92	Solutionâ€Processed Transparent Selfâ€Powered pâ€CuSâ€ZnS/nâ€ZnO UV Photodiode. Physica Status Solidi - Rapid Research Letters, 2018, 12, 1700381.	1.2	54
93	Extremely reduced dielectric confinement in two-dimensional hybrid perovskites with large polar organics. Communications Physics, 2018, 1, .	2.0	135
94	Transmission Electron Microscopy Studies of Transition Metal Oxides Employed as Carrier Selective Contacts in Silicon Solar Cells. , 2018, , .		0
95	23% efficient n-type crystalline silicon solar cells with passivated partial rear contacts. , 2018, , .		1
96	Highly Reliable Superhydrophobic Protection for Organic Field-Effect Transistors by Fluoroalkylsilane-Coated TiO <sub>2</sub> Nanoparticles. ACS Nano, 2018, 12, 11062-11069.	7.3	32
97	Temperature and Humidity Stable Alkali/Alkalineâ€Earth Metal Carbonates as Electron Heterocontacts for Silicon Photovoltaics. Advanced Energy Materials, 2018, 8, 1800743.	10.2	35
98	Zirconium oxide surface passivation of crystalline silicon. Applied Physics Letters, 2018, 112, .	1.5	19
99	A Wearable Microfluidic Sensing Patch for Dynamic Sweat Secretion Analysis. ACS Sensors, 2018, 3, 944-952.	4.0	285
100	Thermal Stability of Hole-Selective Tungsten Oxide: In Situ Transmission Electron Microscopy Study. Scientific Reports, 2018, 8, 12651.	1.6	16
101	Polarization-resolved black phosphorus/molybdenum disulfide mid-wave infrared photodiodes with high detectivity at room temperature. Nature Photonics, 2018, 12, 601-607.	15.6	366
102	Ultrafast Spontaneous Emission from a Slot-Antenna Coupled WSe <sub>2</sub> Monolayer. ACS Photonics, 2018, 5, 2701-2705.	3.2	17
103	Roll-to-Roll Gravure Printed Electrochemical Sensors for Wearable and Medical Devices. ACS Nano, 2018, 12, 6978-6987.	7.3	275
104	Solution-Synthesized High-Mobility Tellurium Nanoflakes for Short-Wave Infrared Photodetectors. ACS Nano, 2018, 12, 7253-7263.	7.3	298
105	Bright Electroluminescence from Back-Gated WSe2 P-N Junctions Using Pulsed Injection. , 2018, , .		0
106	A Low Resistance Calcium/Reduced Titania Passivated Contact for High Efficiency Crystalline Silicon Solar Cells. Advanced Energy Materials, 2017, 7, 1602606.	10.2	97
107	Band Tailing and Deep Defect States in CH <sub>3</sub> NH <sub>3</sub> Pb(I <sub>1–<i>x</i></sub> Br <sub><i>x</i></sub> ) <sub>3</sub> Perovskites As Revealed by Sub-Bandgap Photocurrent. ACS Energy Letters, 2017, 2, 709-715.	8.8	102
108	Analysis of the interface characteristics of CVD-grown monolayer MoS <sub>2</sub> by noise measurements. Nanotechnology, 2017, 28, 145702.	1.3	14

#	Article	IF	CITATIONS
109	Smart Actuators and Adhesives for Reconfigurable Matter. Accounts of Chemical Research, 2017, 50, 691-702.	7.6	151
110	Nanoscience and Nanotechnology Cross Borders. ACS Nano, 2017, 11, 1123-1126.	7.3	4
111	Determining Atomic-Scale Structure and Composition of Organo-Lead Halide Perovskites by Combining High-Resolution X-ray Absorption Spectroscopy and First-Principles Calculations. ACS Energy Letters, 2017, 2, 1183-1189.	8.8	23
112	Autonomous sweat extraction and analysis applied to cystic fibrosis and glucose monitoring using a fully integrated wearable platform. Proceedings of the National Academy of Sciences of the United States of America, 2017, 114, 4625-4630.	3.3	573
113	Highly Stable Near-Unity Photoluminescence Yield in Monolayer MoS <sub>2</sub> by Fluoropolymer Encapsulation and Superacid Treatment. ACS Nano, 2017, 11, 5179-5185.	7.3	86
114	Nanoscale Junction Formation by Gas-Phase Monolayer Doping. ACS Applied Materials & Interfaces, 2017, 9, 20648-20655.	4.0	22
115	Room temperature multiplexed gas sensing using chemical-sensitive 3.5-nm-thin silicon transistors. Science Advances, 2017, 3, e1602557.	4.7	142
116	Wafer-Scale Growth of WSe <sub>2</sub> Monolayers Toward Phase-Engineered Hybrid WO <sub><i>x</i>/i&gt;</sub> /WSe <sub>2</sub> Films with Sub-ppb NO <sub><i>x</i>/i&gt;</sub> Gas Sensing by a Low-Temperature Plasma-Assisted Selenization Process. Chemistry of Materials, 2017, 29, 1587-1598.	3.2	99
117	Mid-Wave Infrared Photoconductors Based on Black Phosphorus-Arsenic Alloys. ACS Nano, 2017, 11, 11724-11731.	7.3	184
118	Low Pressure Vapor-assisted Solution Process for Tunable Band Gap Pinhole-free Methylammonium Lead Halide Perovskite Films. Journal of Visualized Experiments, 2017, , .	0.2	0
119	Wearable Devices: Wearable Microfluidic Diaphragm Pressure Sensor for Health and Tactile Touch Monitoring (Adv. Mater. 39/2017). Advanced Materials, 2017, 29, .	11.1	6
120	Defect passivation of transition metal dichalcogenides via a charge transfer van der Waals interface. Science Advances, 2017, 3, e1701661.	4.7	95
121	Our First and Next Decades at ACS Nano. ACS Nano, 2017, 11, 7553-7555.	7.3	0
122	Efficient solar-driven electrochemical CO <sub>2</sub> reduction to hydrocarbons and oxygenates. Energy and Environmental Science, 2017, 10, 2222-2230.	15.6	145
123	Strain-engineered growth of two-dimensional materials. Nature Communications, 2017, 8, 608.	5.8	253
124	Microchannel contacting of crystalline silicon solar cells. Scientific Reports, 2017, 7, 9085.	1.6	8
125	3D Printed "Earable―Smart Devices for Real-Time Detection of Core Body Temperature. ACS Sensors, 2017, 2, 990-997.	4.0	105
126	Wearable Microfluidic Diaphragm Pressure Sensor for Health and Tactile Touch Monitoring. Advanced Materials, 2017, 29, 1701985.	11.1	431

#	Article	IF	CITATIONS
127	Measuring the Edge Recombination Velocity of Monolayer Semiconductors. Nano Letters, 2017, 17, 5356-5360.	4.5	19
128	High-gain monolithic 3D CMOS inverter using layered semiconductors. Applied Physics Letters, 2017, 111, .	1.5	8
129	Calcium contacts to nâ€ŧype crystalline silicon solar cells. Progress in Photovoltaics: Research and Applications, 2017, 25, 636-644.	4.4	60
130	Conductive and Stable Magnesium Oxide Electronâ€Selective Contacts for Efficient Silicon Solar Cells. Advanced Energy Materials, 2017, 7, 1601863.	10.2	174
131	Measuring the edge recombination velocity of monolayer semiconductors. , 2017, , .		0
132	Superacid-Treated Silicon Surfaces: Extending the Limit of Carrier Lifetime for Photovoltaic Applications. IEEE Journal of Photovoltaics, 2017, 7, 1574-1583.	1.5	40
133	A Big Year Ahead for Nano in 2018. ACS Nano, 2017, 11, 11755-11757.	7.3	1
134	Investigation of InP defect characteristics grown using novel TF-VLS technique. , 2017, , .		0
135	Metal Nanoparticle Hole Contacts for Silicon Solar Cells. , 2017, , .		0
136	2D Semiconductor Optoelectronics. , 2017, , .		1
137	Carbon Nanotubes: Printed Carbon Nanotube Electronics and Sensor Systems (Adv. Mater. 22/2016). Advanced Materials, 2016, 28, 4396-4396.	11.1	8
138	Goldâ€Mediated Exfoliation of Ultralarge Optoelectronicallyâ€Perfect Monolayers. Advanced Materials, 2016, 28, 4053-4058.	11.1	307
139	A Wearable Electrochemical Platform for Noninvasive Simultaneous Monitoring of Ca <sup>2+</sup> and pH. ACS Nano, 2016, 10, 7216-7224.	7.3	480
140	2D materials advances: from large scale synthesis and controlled heterostructures to improved characterization techniques, defects and applications. 2D Materials, 2016, 3, 042001.	2.0	408
141	Nanoscience and Nanotechnology Impacting Diverse Fields of Science, Engineering, and Medicine. ACS Nano, 2016, 10, 10615-10617.	7.3	22
142	2D-2D tunneling field-effect transistors using WSe2/SnSe2 heterostructures. Applied Physics Letters, 2016, 108, .	1.5	252
143	Survey of dopant-free carrier-selective contacts for silicon solar cells. , 2016, , .		12
144	Improved photoswitching response times of MoS2 field-effect transistors by stacking <i>p</i> -type copper phthalocyanine layer. Applied Physics Letters, 2016, 109, .	1.5	29

#	Article	IF	CITATIONS
145	Wearable sweat biosensors. , 2016, , .		20
146	Wearable Microsensor Array for Multiplexed Heavy Metal Monitoring of Body Fluids. ACS Sensors, 2016, 1, 866-874.	4.0	297
147	MoS <sub>2</sub> transistors with 1-nanometer gate lengths. Science, 2016, 354, 99-102.	6.0	1,140
148	Application of 3D Printing for Smart Objects with Embedded Electronic Sensors and Systems. Advanced Materials Technologies, 2016, 1, 1600013.	3.0	167
149	Superacid Passivation of Crystalline Silicon Surfaces. ACS Applied Materials & amp; Interfaces, 2016, 8, 24205-24211.	4.0	38
150	Compliant substrate epitaxy: Au on <mml:math xmlns:mml="http://www.w3.org/1998/Math/MathML"&gt;<mml:msub><mml:mi>MoS</mml:mi><mml:mn>2Physical Review B, 2016, 93, .</mml:mn></mml:msub></mml:math 	m <b>a.ı</b> <td>nl:m2sub&gt;</td>	nl:m2sub>
151	Defective TiO2 with high photoconductive gain for efficient and stable planar heterojunction perovskite solar cells. Nature Communications, 2016, 7, 12446.	5.8	139
152	Efficient silicon solar cells with dopant-free asymmetric heterocontacts. Nature Energy, 2016, 1, .	19.8	461
153	Fully gravure printed complementary carbon nanotube TFTs for a clock signal generator using an epoxy-imine based cross-linker as an n-dopant and encapsulant. Nanoscale, 2016, 8, 19876-19881.	2.8	19
154	Origin of multi-level switching and telegraphic noise in organic nanocomposite memory devices. Scientific Reports, 2016, 6, 33967.	1.6	21
155	Illâ€Vs at scale: a PV manufacturing cost analysis of the thin film vapor–liquid–solid growth mode. Progress in Photovoltaics: Research and Applications, 2016, 24, 871-878.	4.4	20
156	Printed Carbon Nanotube Electronics and Sensor Systems. Advanced Materials, 2016, 28, 4397-4414.	11.1	369
157	Increased Optoelectronic Quality and Uniformity of Hydrogenated p-InP Thin Films. Chemistry of Materials, 2016, 28, 4602-4607.	3.2	12
158	General Thermal Texturization Process of MoS <sub>2</sub> for Efficient Electrocatalytic Hydrogen Evolution Reaction. Nano Letters, 2016, 16, 4047-4053.	4.5	106
159	Air-Stable n-Doping of WSe <sub>2</sub> by Anion Vacancy Formation with Mild Plasma Treatment. ACS Nano, 2016, 10, 6853-6860.	7.3	202
160	Magnesium Fluoride Electron-Selective Contacts for Crystalline Silicon Solar Cells. ACS Applied Materials & Interfaces, 2016, 8, 14671-14677.	4.0	188
161	High Luminescence Efficiency in MoS <sub>2</sub> Grown by Chemical Vapor Deposition. ACS Nano, 2016, 10, 6535-6541.	7.3	140
162	Monolithic 3D CMOS Using Layered Semiconductors. Advanced Materials, 2016, 28, 2547-2554.	11.1	107

#	Article	IF	CITATIONS
163	Lithium Fluoride Based Electron Contacts for High Efficiency nâ€Type Crystalline Silicon Solar Cells. Advanced Energy Materials, 2016, 6, 1600241.	10.2	134
164	Fully integrated wearable sensor arrays for multiplexed in situ perspiration analysis. Nature, 2016, 529, 509-514.	13.7	3,508
165	Electrical Properties of Synthesized Large-Area MoS2 Field-Effect Transistors Fabricated with Inkjet-Printed Contacts. ACS Nano, 2016, 10, 2819-2826.	7.3	64
166	Recombination Kinetics and Effects of Superacid Treatment in Sulfur- and Selenium-Based Transition Metal Dichalcogenides. Nano Letters, 2016, 16, 2786-2791.	4.5	233
167	Chemical Bath Deposition of p-Type Transparent, Highly Conducting (CuS) <sub><i>x</i></sub> :(ZnS) <sub>1–<i>x</i></sub> Nanocomposite Thin Films and Fabrication of Si Heterojunction Solar Cells. Nano Letters, 2016, 16, 1925-1932.	4.5	89
168	Direct growth of single-crystalline III–V semiconductors on amorphous substrates. Nature Communications, 2016, 7, 10502.	5.8	45
169	High Photoluminescence Quantum Yield in Band Gap Tunable Bromide Containing Mixed Halide Perovskites. Nano Letters, 2016, 16, 800-806.	4.5	269
170	2D layered materials: From materials properties to device applications. , 2015, , .		9
171	A fully roll-to-roll gravure-printed carbon nanotube-based active matrix for multi-touch sensors. Scientific Reports, 2015, 5, 17707.	1.6	96
172	Fully printed flexible and disposable wireless cyclic voltammetry tag. Scientific Reports, 2015, 5, 8105.	1.6	61
173	Electron-Selective TiO2 Contact for Cu(In,Ga)Se2 Solar Cells. Scientific Reports, 2015, 5, 16028.	1.6	52
174	Room Temperature Oxide Deposition Approach to Fully Transparent, Allâ€Oxide Thinâ€Film Transistors. Advanced Materials, 2015, 27, 6090-6095.	11.1	57
175	Frontispiece: Enhanced Photocatalytic Reduction of CO2to CO through TiO2Passivation of InP in Ionic Liquids. Chemistry - A European Journal, 2015, 21, n/a-n/a.	1.7	0
176	Enhanced Photocatalytic Reduction of CO <sub>2</sub> to CO through TiO <sub>2</sub> Passivation of InP in Ionic Liquids. Chemistry - A European Journal, 2015, 21, 13502-13507.	1.7	52
177	Thinâ€Film Solar Cells with InP Absorber Layers Directly Grown on Nonepitaxial Metal Substrates. Advanced Energy Materials, 2015, 5, 1501337.	10.2	13
178	Photoluminescence imaging characterization of thin-film InP. , 2015, , .		4
179	Grand Plans for Nano. ACS Nano, 2015, 9, 11503-11505.	7.3	3
180	Integrated Manufacture of Exoskeletons and Sensing Structures for Folded Millirobots. Journal of Mechanisms and Robotics, 2015, 7, .	1.5	38

#	Article	IF	CITATIONS
181	Role of TiO <sub>2</sub> Surface Passivation on Improving the Performance of p-InP Photocathodes. Journal of Physical Chemistry C, 2015, 119, 2308-2313.	1.5	127
182	Dual-Gated MoS <sub>2</sub> /WSe <sub>2</sub> van der Waals Tunnel Diodes and Transistors. ACS Nano, 2015, 9, 2071-2079.	7.3	560
183	Largeâ€Area Compliant Tactile Sensors Using Printed Carbon Nanotube Activeâ€Matrix Backplanes. Advanced Materials, 2015, 27, 1561-1566.	11.1	198
184	Engineering Light Outcoupling in 2D Materials. Nano Letters, 2015, 15, 1356-1361.	4.5	138
185	Enabling unassisted solar water splitting by iron oxide and silicon. Nature Communications, 2015, 6, 7447.	5.8	429
186	Quantum Well InAs/AlSb/GaSb Vertical Tunnel FET With HSQ Mechanical Support. IEEE Nanotechnology Magazine, 2015, 14, 580-584.	1.1	19
187	MoS2 Heterojunctions by Thickness Modulation. Scientific Reports, 2015, 5, 10990.	1.6	93
188	Nonepitaxial Thin-Film InP for Scalable and Efficient Photocathodes. Journal of Physical Chemistry Letters, 2015, 6, 2177-2182.	2.1	33
189	Catalyst-dependent morphological evolution by interfacial stress in crystalline–amorphous core–shell germanium nanowires. RSC Advances, 2015, 5, 28454-28459.	1.7	1
190	Artificial Photosynthesis on TiO <sub>2</sub> -Passivated InP Nanopillars. Nano Letters, 2015, 15, 6177-6181.	4.5	86
191	Oriented Growth of Gold Nanowires on MoS <sub>2</sub> . Advanced Functional Materials, 2015, 25, 6257-6264.	7.8	21
192	Mimicking the Human Brain and More: New Grand Challenge Initiatives. ACS Nano, 2015, 9, 10533-10536.	7.3	5
193	Near-unity photoluminescence quantum yield in MoS <sub>2</sub> . Science, 2015, 350, 1065-1068.	6.0	993
194	Highly Uniform and Stable n-Type Carbon Nanotube Transistors by Using Positively Charged Silicon Nitride Thin Films. Nano Letters, 2015, 15, 392-397.	4.5	92
195	Photovoltaic Material Characterization With Steady State and Transient Photoluminescence. IEEE Journal of Photovoltaics, 2015, 5, 282-287.	1.5	15
196	Enhanced Spontaneous Emission from an Optical Antenna Coupled WSe2 Monolayer. , 2015, , .		3
197	Enhanced Nearâ€Bandgap Response in InP Nanopillar Solar Cells. Advanced Energy Materials, 2014, 4, 1400061.	10.2	21
198	Air stable <i>n</i> -doping of WSe2 by silicon nitride thin films with tunable fixed charge density. APL Materials, 2014, 2, .	2.2	76

#	Article	IF	CITATIONS
199	Fermi level stabilization and band edge energies in CdxZn1â^'xO alloys. Journal of Applied Physics, 2014, 115, .	1.1	37
200	A Year for Nanoscience. ACS Nano, 2014, 8, 11901-11903.	7.3	6
201	Silicon heterojunction solar cell with passivated hole selective MoOx contact. Applied Physics Letters, 2014, 104, .	1.5	363
202	Strong interlayer coupling in van der Waals heterostructures built from single-layer chalcogenides. Proceedings of the National Academy of Sciences of the United States of America, 2014, 111, 6198-6202.	3.3	970
203	Field-Effect Transistors Built from All Two-Dimensional Material Components. ACS Nano, 2014, 8, 6259-6264.	7.3	582
204	Air-Stable Surface Charge Transfer Doping of MoS <sub>2</sub> by Benzyl Viologen. Journal of the American Chemical Society, 2014, 136, 7853-7856.	6.6	593
205	Highly sensitive electronic whiskers based on patterned carbon nanotube and silver nanoparticle composite films. Proceedings of the National Academy of Sciences of the United States of America, 2014, 111, 1703-1707.	3.3	234
206	Hole Contacts on Transition Metal Dichalcogenides: Interface Chemistry and Band Alignments. ACS Nano, 2014, 8, 6265-6272.	7.3	173
207	Efficient and Sustained Photoelectrochemical Water Oxidation by Cobalt Oxide/Silicon Photoanodes with Nanotextured Interfaces. Journal of the American Chemical Society, 2014, 136, 6191-6194.	6.6	204
208	Photoactuators and motors based on carbon nanotubes with selective chirality distributions. Nature Communications, 2014, 5, 2983.	5.8	269
209	Hole Selective MoO <sub><i>x</i></sub> Contact for Silicon Solar Cells. Nano Letters, 2014, 14, 967-971.	4.5	476
210	Electrodeposition of High-Purity Indium Thin Films and Its Application to Indium Phosphide Solar Cells. Journal of the Electrochemical Society, 2014, 161, D794-D800.	1.3	16
211	Air Stable p-Doping of WSe <sub>2</sub> by Covalent Functionalization. ACS Nano, 2014, 8, 10808-10814.	7.3	208
212	MoS <sub>2</sub> P-type Transistors and Diodes Enabled by High Work Function MoO <sub><i>x</i></sub> Contacts. Nano Letters, 2014, 14, 1337-1342.	4.5	487
213	Series resistance and mobility in mechanically-exfoliated layered transition metal dichalcogenide MOSFETs. , 2014, , .		2
214	Performance Enhancement of a Graphene-Zinc Phosphide Solar Cell Using the Electric Field-Effect. Nano Letters, 2014, 14, 4280-4285.	4.5	45
215	Deterministic Nucleation of InP on Metal Foils with the Thin-Film Vapor–Liquid–Solid Growth Mode. Chemistry of Materials, 2014, 26, 1340-1344.	3.2	32
216	Design of Surfactant–Substrate Interactions for Roll-to-Roll Assembly of Carbon Nanotubes for Thin-Film Transistors. Journal of the American Chemical Society, 2014, 136, 11188-11194.	6.6	60

#	Article	IF	CITATIONS
217	Highly deformable liquid-state heterojunction sensors. Nature Communications, 2014, 5, 5032.	5.8	221
218	BiVO <sub>4</sub> thin film photoanodes grown by chemical vapor deposition. Physical Chemistry Chemical Physics, 2014, 16, 1651-1657.	1.3	77
219	High-Gain Inverters Based on WSe <sub>2</sub> Complementary Field-Effect Transistors. ACS Nano, 2014, 8, 4948-4953.	7.3	284
220	Strain-Induced Indirect to Direct Bandgap Transition in Multilayer WSe <sub>2</sub> . Nano Letters, 2014, 14, 4592-4597.	4.5	572
221	19.2% Efficient InP Heterojunction Solar Cell with Electron-Selective TiO <sub>2</sub> Contact. ACS Photonics, 2014, 1, 1245-1250.	3.2	116
222	Highly Stable Hysteresis-Free Carbon Nanotube Thin-Film Transistors by Fluorocarbon Polymer Encapsulation. ACS Applied Materials & Interfaces, 2014, 6, 8441-8446.	4.0	87
223	Vertically aligned tungsten oxide nanorod film with enhanced performance in photoluminescence humidity sensing. Sensors and Actuators B: Chemical, 2014, 202, 708-713.	4.0	27
224	User-interactive electronic skin for instantaneous pressure visualization. Nature Materials, 2013, 12, 899-904.	13.3	1,044
225	Fully Printed, High Performance Carbon Nanotube Thin-Film Transistors on Flexible Substrates. Nano Letters, 2013, 13, 3864-3869.	4.5	372
226	Two-dimensional to three-dimensional tunneling in InAs/AlSb/GaSb quantum well heterojunctions. Journal of Applied Physics, 2013, 114, .	1.1	16
227	Uncovering the intrinsic size dependence of hydriding phase transformations in nanocrystals. Nature Materials, 2013, 12, 905-912.	13.3	116
228	Surface Charge Transfer Doping of III–V Nanostructures. Journal of Physical Chemistry C, 2013, 117, 17845-17849.	1.5	19
229	Short-Channel Transistors Constructed with Solution-Processed Carbon Nanotubes. ACS Nano, 2013, 7, 798-803.	7.3	83
230	Reactive Sputtering of Bismuth Vanadate Photoanodes for Solar Water Splitting. Journal of Physical Chemistry C, 2013, 117, 21635-21642.	1.5	162
231	Be Critical but Fair. ACS Nano, 2013, 7, 8313-8316.	7.3	5
232	Exciting Times for Nano. ACS Nano, 2013, 7, 10437-10439.	7.3	1
233	Spin-On Organic Polymer Dopants for Silicon. Journal of Physical Chemistry Letters, 2013, 4, 3741-3746.	2.1	51
234	Carbon Nanotube Active-Matrix Backplanes for Mechanically Flexible Visible Light and X-ray Imagers. Nano Letters, 2013, 13, 5425-5430.	4.5	86

#	Article	IF	CITATIONS
235	Ballistic InAs Nanowire Transistors. Nano Letters, 2013, 13, 555-558.	4.5	155
236	Amorphous Si Thin Film Based Photocathodes with High Photovoltage for Efficient Hydrogen Production. Nano Letters, 2013, 13, 5615-5618.	4.5	151
237	Influence of catalyst choices on transport behaviors of InAs NWs for high-performance nanoscale transistors. Physical Chemistry Chemical Physics, 2013, 15, 2654.	1.3	17
238	Carbon nanotube electronics – moving forward. Chemical Society Reviews, 2013, 42, 2592-2609.	18.7	276
239	High quality interfaces of InAs-on-insulator field-effect transistors with ZrO2 gate dielectrics. Applied Physics Letters, 2013, 102, .	1.5	33
240	Degenerate n-Doping of Few-Layer Transition Metal Dichalcogenides by Potassium. Nano Letters, 2013, 13, 1991-1995.	4.5	651
241	Near-ideal electrical properties of InAs/WSe2 van der Waals heterojunction diodes. Applied Physics Letters, 2013, 102, .	1.5	71
242	Quantum membranes: A new materials platform for future electronics. , 2013, , .		0
243	Effects of palladium coating on field-emission properties of carbon nanofibers in a hydrogen plasma. Thin Solid Films, 2013, 534, 488-491.	0.8	11
244	Carbon nanotube macroelectronics: toward system-on-plastic. Proceedings of SPIE, 2013, , .	0.8	0
245	Solar fuels production by artificial photosynthesis. , 2013, , .		0
246	A direct thin-film path towards low-cost large-area III-V photovoltaics. Scientific Reports, 2013, 3, 2275.	1.6	65
247	Quantum of optical absorption in two-dimensional semiconductors. Proceedings of the National Academy of Sciences of the United States of America, 2013, 110, 11688-11691.	3.3	75
248	Contact printing of compositionally graded CdS <sub><i>x</i></sub> Se <sub>1â~<i>x</i></sub> nanowire parallel arrays for tunable photodetectors. Nanotechnology, 2012, 23, 045201.	1.3	58
249	Multifunctional, flexible electronic systems based on engineered nanostructured materials. Nanotechnology, 2012, 23, 344001.	1.3	38
250	A compact neutron generator using a field ionization source. Review of Scientific Instruments, 2012, 83, 02B312.	0.6	14
251	Comparative study of solution-processed carbon nanotube network transistors. Applied Physics Letters, 2012, 101, 112104.	1.5	30
252	Morphological and spatial control of InP growth using closed-space sublimation. Journal of Applied Physics, 2012, 112, 123102.	1.1	18

#	Article	IF	CITATIONS
253	We Take It Personally. ACS Nano, 2012, 6, 10417-10419.	7.3	3
254	Observation of Degenerate One-Dimensional Sub-Bands in Cylindrical InAs Nanowires. Nano Letters, 2012, 12, 1340-1343.	4.5	65
255	Nanoscale InGaSb Heterostructure Membranes on Si Substrates for High Hole Mobility Transistors. Nano Letters, 2012, 12, 2060-2066.	4.5	85
256	Measuring Academic Impact. ACS Nano, 2012, 6, 6529-6529.	7.3	2
257	Self-Aligned, Extremely High Frequency Ill–V Metal-Oxide-Semiconductor Field-Effect Transistors on Rigid and Flexible Substrates. Nano Letters, 2012, 12, 4140-4145.	4.5	73
258	High optical quality polycrystalline indium phosphide grown on metal substrates by metalorganic chemical vapor deposition. Journal of Applied Physics, 2012, 111, 123112.	1.1	21
259	Nanopillar photovoltaics: Materials, processes, and devices. Nano Energy, 2012, 1, 132-144.	8.2	142
260	pâ€Type InP Nanopillar Photocathodes for Efficient Solarâ€Driven Hydrogen Production. Angewandte Chemie - International Edition, 2012, 51, 10760-10764.	7.2	245
261	Extremely Bendable, High-Performance Integrated Circuits Using Semiconducting Carbon Nanotube Networks for Digital, Analog, and Radio-Frequency Applications. Nano Letters, 2012, 12, 1527-1533.	4.5	292
262	III–V Complementary Metal–Oxide–Semiconductor Electronics on Silicon Substrates. Nano Letters, 2012, 12, 3592-3595.	4.5	80
263	Recycling Is Not Always Good: The Dangers of Self-Plagiarism. ACS Nano, 2012, 6, 1-4.	7.3	49
264	Quantum Size Effects on the Chemical Sensing Performance of Two-Dimensional Semiconductors. Journal of Physical Chemistry C, 2012, 116, 9750-9754.	1.5	41
265	High-Performance Single Layered WSe <sub>2</sub> p-FETs with Chemically Doped Contacts. Nano Letters, 2012, 12, 3788-3792.	4.5	1,547
266	Ultrathin-Body High-Mobility InAsSb-on-Insulator Field-Effect Transistors. IEEE Electron Device Letters, 2012, 33, 504-506.	2.2	28
267	Low-Resistance Electrical Contact to Carbon Nanotubes With Graphitic Interfacial Layer. IEEE Transactions on Electron Devices, 2012, 59, 12-19.	1.6	105
268	Development of a compact neutron source based on field ionization processes. Journal of Vacuum Science and Technology B:Nanotechnology and Microelectronics, 2011, 29, 02B107.	0.6	16
269	Optically- and Thermally-Responsive Programmable Materials Based on Carbon Nanotube-Hydrogel Polymer Composites. Nano Letters, 2011, 11, 3239-3244.	4.5	476
270	Roll-to-Roll Anodization and Etching of Aluminum Foils for High-Throughput Surface Nanotexturing. Nano Letters, 2011, 11, 3425-3430.	4.5	58

#	Article	IF	CITATIONS
271	ACS Nano in 2011 and Looking Forward to 2012. ACS Nano, 2011, 5, 9301-9302.	7.3	Ο
272	Strongly enhanced minority lifetimes in single silicon nanowires by surface passivation. , 2011, , .		0
273	Dramatic Reduction of Surface Recombination by in Situ Surface Passivation of Silicon Nanowires. Nano Letters, 2011, 11, 2527-2532.	4.5	230
274	Carbon Nanotube Active-Matrix Backplanes for Conformal Electronics and Sensors. Nano Letters, 2011, 11, 5408-5413.	4.5	270
275	Quantum Confinement Effects in Nanoscale-Thickness InAs Membranes. Nano Letters, 2011, 11, 5008-5012.	4.5	97
276	Power surfing on waves. Nature, 2011, 472, 304-305.	13.7	3
277	Nanoscale Bipolar and Complementary Resistive Switching Memory Based on Amorphous Carbon. IEEE Transactions on Electron Devices, 2011, 58, 3933-3939.	1.6	78
278	Nanoscale Semiconductor "X―on Substrate "Y―– Processes, Devices, and Applications. Advanced Materials, 2011, 23, 3115-3127.	11.1	42
279	Rationally Designed, Threeâ€Dimensional Carbon Nanotube Backâ€Contacts for Efficient Solar Devices. Advanced Energy Materials, 2011, 1, 1040-1045.	10.2	27
280	Molecular monolayers for conformal, nanoscale doping of InP nanopillar photovoltaics. Applied Physics Letters, 2011, 98, .	1.5	54
281	Benchmarking the performance of ultrathin body InAs-on-insulator transistors as a function of body thickness. Applied Physics Letters, 2011, 99, .	1.5	40
282	Strain engineering of epitaxially transferred, ultrathin layers of III-V semiconductor on insulator. Applied Physics Letters, 2011, 98, 012111.	1.5	23
283	Ultrathin body InAs tunneling field-effect transistors on Si substrates. Applied Physics Letters, 2011, 98, .	1.5	76
284	PCBM-Grafted MWNT for Enhanced Electron Transport in Polymer Solar Cells. Journal of the Electrochemical Society, 2011, 158, A237.	1.3	8
285	Patterned p-Doping of InAs Nanowires by Gas-Phase Surface Diffusion of Zn. Nano Letters, 2010, 10, 509-513.	4.5	57
286	Thermoresponsive Chemical Connectors Based on Hybrid Nanowire Forests. Angewandte Chemie - International Edition, 2010, 49, 616-619.	7.2	29
287	Palladium/silicon nanowire Schottky barrier-based hydrogen sensors. Sensors and Actuators B: Chemical, 2010, 145, 232-238.	4.0	124
288	Flexible Carbonâ€Nanofiber Connectors with Anisotropic Adhesion Properties. Small, 2010, 6, 22-26.	5.2	44

#	Article	IF	CITATIONS
289	Ultrathin compound semiconductor on insulator layers for high-performance nanoscale transistors. Nature, 2010, 468, 286-289.	13.7	373
290	Nanowire active-matrix circuitry for low-voltage macroscale artificial skin. Nature Materials, 2010, 9, 821-826.	13.3	1,162
291	Design constraints and guidelines for CdS/CdTe nanopillar based photovoltaics. Applied Physics Letters, 2010, 96, .	1.5	78
292	Graphitic interfacial layer to carbon nanotube for low electrical contact resistance. , 2010, , .		5
293	Preface to Special Topic: Selected Papers from the International Conference on Flexible and Printed Electronics, Jeju Island, Korea, 2009. Journal of Applied Physics, 2010, 108, 102701.	1.1	2
294	Hierarchical polymer micropillar arrays decorated with ZnO nanowires. Nanotechnology, 2010, 21, 295305.	1.3	30
295	Nanoscale Structural Engineering via Phase Segregation: Auâ^'Ge System. Nano Letters, 2010, 10, 393-397.	4.5	23
296	Shape-Controlled Synthesis of Single-Crystalline Nanopillar Arrays by Template-Assisted Vaporâ^'Liquidâ^'Solid Process. Journal of the American Chemical Society, 2010, 132, 13972-13974.	6.6	29
297	Parallel Array InAs Nanowire Transistors for Mechanically Bendable, Ultrahigh Frequency Electronics. ACS Nano, 2010, 4, 5855-5860.	7.3	105
298	Ordered Arrays of Dual-Diameter Nanopillars for Maximized Optical Absorption. Nano Letters, 2010, 10, 3823-3827.	4.5	269
299	Black Ge Based on Crystalline/Amorphous Core/Shell Nanoneedle Arrays. Nano Letters, 2010, 10, 520-523.	4.5	68
300	Direct Chemical Vapor Deposition of Graphene on Dielectric Surfaces. Nano Letters, 2010, 10, 1542-1548.	4.5	439
301	Metal-catalyzed crystallization of amorphous carbon to graphene. Applied Physics Letters, 2010, 96, .	1.5	234
302	Resistive switching of carbon-based RRAM with CNT electrodes for ultra-dense memory. , 2010, , .		4
303	Prospect of tunneling green transistor for 0.1V CMOS. , 2010, , .		61
304	Nanowire-based 2-D and 3-D XoY electronics. , 2010, , .		0
305	Hybrid core-multishell nanowire forests for electrical connector applications. Applied Physics Letters, 2009, 94, 263110.	1.5	28
306	Monolayer doping and diameter-dependent electron mobility assessment of nanowires. , 2009, , .		4

Monolayer doping and diameter-dependent electron mobility assessment of nanowires. , 2009, , . 306

#	Article	IF	CITATIONS
307	Nanoscale doping of InAs via sulfur monolayers. Applied Physics Letters, 2009, 95, .	1.5	71
308	Wet and Dry Adhesion Properties of Self‣elective Nanowire Connectors. Advanced Functional Materials, 2009, 19, 3098-3102.	7.8	31
309	Toward the Development of Printable Nanowire Electronics and Sensors. Advanced Materials, 2009, 21, 3730-3743.	11.1	363
310	Challenges and prospects of nanopillar-based solar cells. Nano Research, 2009, 2, 829.	5.8	223
311	Three-dimensional nanopillar-array photovoltaics on low-cost and flexible substrates. Nature Materials, 2009, 8, 648-653.	13.3	997
312	Wafer-Scale, Sub-5 nm Junction Formation by Monolayer Doping and Conventional Spike Annealing. Nano Letters, 2009, 9, 725-730.	4.5	148
313	Carbon Nanotube Field-Effect Transistors. Integrated Circuits and Systems, 2009, , 63-86.	0.2	1
314	Diameter-Dependent Electron Mobility of InAs Nanowires. Nano Letters, 2009, 9, 360-365.	4.5	353
315	Hybrid Coreâ^'Shell Nanowire Forests as Self-Selective Chemical Connectors. Nano Letters, 2009, 9, 2054-2058.	4.5	59
316	Monolayer Resist for Patterned Contact Printing of Aligned Nanowire Arrays. Journal of the American Chemical Society, 2009, 131, 2102-2103.	6.6	70
317	Synthesis, contact printing, and device characterization of Ni-catalyzed, crystalline InAs nanowires. Nano Research, 2008, 1, 32-39.	5.8	70
318	Phosphine Oxide Monolayers on SiO <sub>2</sub> Surfaces. Angewandte Chemie - International Edition, 2008, 47, 4440-4442.	7.2	37
319	Controlled nanoscale doping of semiconductors via molecular monolayers. Nature Materials, 2008, 7, 62-67.	13.3	311
320	Solar cells on curtains. Nature Materials, 2008, 7, 835-836.	13.3	37
321	Wafer-Scale Assembly of Highly Ordered Semiconductor Nanowire Arrays by Contact Printing. Nano Letters, 2008, 8, 20-25.	4.5	542
322	The 2008 Kavli Prize in Nanoscience: Carbon Nanotubes. ACS Nano, 2008, 2, 1329-1335.	7.3	48
323	Large-scale, heterogeneous integration of nanowire arrays for image sensor circuitry. Proceedings of the United States of America, 2008, 105, 11066-11070.	3.3	233
324	Formation and Characterization of NixInAs/InAs Nanowire Heterostructures by Solid Source Reaction. Nano Letters, 2008, 8, 4528-4533.	4.5	61

#	Article	IF	CITATIONS
325	Large scale, highly ordered assembly of nanowire parallel arrays by differential roll printing. Applied Physics Letters, 2007, 91, .	1.5	117
326	Generic Nanomaterial Positioning by Carrier and Stationary Phase Design. Nano Letters, 2007, 7, 2764-2768.	4.5	23
327	Layer-by-Layer Assembly of Nanowires for Three-Dimensional, Multifunctional Electronics. Nano Letters, 2007, 7, 773-777.	4.5	573
328	ELECTRICAL TRANSPORT PROPERTIES AND FIELD EFFECT TRANSISTORS OF CARBON NANOTUBES. Nano, 2006, 01, 1-13.	0.5	142
329	Carbon Nanotubes: From Growth, Placement and Assembly Control to 60mV/decade and Sub-60 mV/decade Tunnel Transistors. , 2006, , .		14
330	Self-aligned 40-nm channel carbon nanotube field-effect transistors with subthreshold swings down to 70 mV/decade. , 2005, , .		1
331	Ultra-high-yield growth of vertical single-walled carbon nanotubes: Hidden roles of hydrogen and oxygen. Proceedings of the National Academy of Sciences of the United States of America, 2005, 102, 16141-16145.	3.3	403
332	Regular Arrays of 2 nm Metal Nanoparticles for Deterministic Synthesis of Nanomaterials. Journal of the American Chemical Society, 2005, 127, 11942-11943.	6.6	95
333	High Performance n-Type Carbon Nanotube Field-Effect Transistors with Chemically Doped Contacts. Nano Letters, 2005, 5, 345-348.	4.5	453
334	Electrical contacts to carbon nanotubes down to 1nm in diameter. Applied Physics Letters, 2005, 87, 173101.	1.5	205
335	Ten- to 50-nm-long quasi-ballistic carbon nanotube devices obtained without complex lithography. Proceedings of the National Academy of Sciences of the United States of America, 2004, 101, 13408-13410.	3.3	134
336	High-Field Quasiballistic Transport in Short Carbon Nanotubes. Physical Review Letters, 2004, 92, 106804.	2.9	543
337	Monolithic Integration of Carbon Nanotube Devices with Silicon MOS Technology. Nano Letters, 2004, 4, 123-127.	4.5	131
338	Self-Aligned Ballistic Molecular Transistors and Electrically Parallel Nanotube Arrays. Nano Letters, 2004, 4, 1319-1322.	4.5	505
339	Carbon Nanotube Field-Effect Transistors with Integrated Ohmic Contacts and High-κ Gate Dielectrics. Nano Letters, 2004, 4, 447-450.	4.5	498
340	Miniature Organic Transistors with Carbon Nanotubes as Quasi-One-Dimensional Electrodes. Journal of the American Chemical Society, 2004, 126, 11774-11775.	6.6	184
341	Preferential Growth of Semiconducting Single-Walled Carbon Nanotubes by a Plasma Enhanced CVD Method. Nano Letters, 2004, 4, 317-321.	4.5	485
342	Ballistic carbon nanotube field-effect transistors. Nature, 2003, 424, 654-657.	13.7	2,883

#	Article	IF	CITATIONS
343	Toward Large Arrays of Multiplex Functionalized Carbon Nanotube Sensors for Highly Sensitive and Selective Molecular Detection. Nano Letters, 2003, 3, 347-351.	4.5	953
344	Ballistic Transport in Metallic Nanotubes with Reliable Pd Ohmic Contacts. Nano Letters, 2003, 3, 1541-1544.	4.5	416
345	Efficient Formation of Iron Nanoparticle Catalysts on Silicon Oxide by Hydroxylamine for Carbon Nanotube Synthesis and Electronics. Nano Letters, 2003, 3, 157-161.	4.5	90
346	Germanium nanowire field-effect transistors with SiO2 and high-κ HfO2 gate dielectrics. Applied Physics Letters, 2003, 83, 2432-2434.	1.5	424
347	Hysteresis Caused by Water Molecules in Carbon Nanotube Field-Effect Transistors. Nano Letters, 2003, 3, 193-198.	4.5	890
348	Integration of suspended carbon nanotube arrays into electronic devices and electromechanical systems. Applied Physics Letters, 2002, 81, 913-915.	1.5	237
349	Electrical properties and devices of large-diameter single-walled carbon nanotubes. Applied Physics Letters, 2002, 80, 1064-1066.	1.5	118
350	Carbon Nanotube Transistor Arrays for Multistage Complementary Logic and Ring Oscillators. Nano Letters, 2002, 2, 929-932.	4.5	325
351	High-κ dielectrics for advanced carbon-nanotube transistors and logic gates. Nature Materials, 2002, 1, 241-246.	13.3	928
352	Patterned growth of single-walled carbon nanotubes on full 4-inch wafers. Applied Physics Letters, 2001, 79, 4571-4573.	1.5	195
353	Polymer Functionalization for Air-Stable n-Type Carbon Nanotube Field-Effect Transistors. Journal of the American Chemical Society, 2001, 123, 11512-11513.	6.6	570